N94-20515

10 GHz $YBa_2Cu_3O_{7-\delta}$ superconducting ring resonators on $NdGaO_3$ substrates

H Y To†, G J Valco† and K B Bhasin‡

† Department of Electrical Engineering, Ohio State University, Columbus, Ohio 43210, USA

‡ National Aeronautics and Space Administration, Lewis Research Center, Cleveland, Ohio 44135, USA

Abstract. $YBa_2Cu_3O_{7-\delta}$ thin films were formed on $NdGaO_3$ substrates by laser ablation. Critical temperatures greater than 89 K and critical current densities exceeding 2×10^6 A cm^{-2} at 77 K were obtained. The microwave performance of films patterned into microstrip ring resonators with gold ground planes was measured. An unloaded quality factor six times larger than a that of a gold resonator of identical geometry was achieved. The unloaded quality factor decreased below 70 K for both the superconducting and gold resonators due to increasing dielectric losses in the substrate. The temperature dependence of the loss tangent of $NdGaO_3$ was extracted from the measurements.

1. Introduction

A major area of interest for application of high-temperature superconductors is microwave electronics. The characterization of these materials at microwave frequencies is important for understanding their potential for practical use. Strontium titanate ($SrTiO_3$), a cubic pervoskite, has been used as a substrate for the formation of a thin film of high-temperature superconductor [1] and films on $SrTiO_3$ have among the best DC properties. However, its large dielectric constant and loss tangent make it unsuitable for microwave applications.

Lanthanum aluminate ($LaAlO_3$), which has a similar structure to $SrTiO_3$, has been widely used as the substrate for microwave applications of thin film $YBa_2Cu_3O_{7-\delta}$ (YBCO). This substrate has a lattice mismatch with YBCO of less than one per cent. $LaAlO_3$ has a loss tangent of less than 10^{-4} at 10 GHz [2] and a dielectric constant of 24.5 [3] below the critical temperature (T_c) of YBCO. However, $LaAlO_3$ has a second-order phase transition around 500°C [4]. This causes the substrate to have a high density of twinning and may have a detrimental effect on the microwave performance of the YBCO films.

A search for crystals with similar lattice dimensions reveals that neodymium gallate ($NdGaO_3$) is a promising substrate [4, 5]. $NdGaO_3$ is a perovskite which has about 0.8% lattice mismatch with the YBCO superconductor. Furthermore, the dielectric constant of $NdGaO_3$ is comparable to that of $LaAlO_3$, and this crystal is twin free [6, 7]. The crystal has a second-order phase transition at 950°C which is higher than the typical processing temperature of *in situ* annealed high-temperature superconductors.

Recently, there have been reports on the growth of epitaxial YBCO films on $NdGaO_3$ [8, 9, 10]. The microwave properties of YBCO superconducting films deposited on $NdGaO_3$ have been measured by other researchers [11]. However, to our knowledge, no measurements on resonators fabricated using the YBCO film on $NdGaO_3$ have been reported at frequencies higher than 5 GHz or as a function of temperature.

In this report, YBCO superconducting thin films were deposited on (001) $NdGaO_3$ and patterned into ring resonators. The advantage of a ring resonator over a linear resonator is that the ring resonator does not have radiation losses from an open end. The reflection coefficients of the resonator were measured as a function of temperature. The unloaded quality factors at 10 GHz were calculated and the effective surface resistance was extracted from the loaded Q-factors. Further, the loss tangent of $NdGaO_3$ was determined as a function of temperature.

2. Sample preparation

A two-inch (5.1 cm) diameter, 20 mils (0.51 mm) thick, (001) $NdGaO_3$ substrate, polished on both sides, was cut into typical sizes of 1 cm x 1 cm and 0.8 cm by 0.4 cm for microwave and DC transport characterization, respectively. YBCO thin films were deposited on to the substrates by laser ablation. Prior to deposition of the films, the substrates were cleaned in acetone and methanol with ultrasonic agitation for 5 minutes each. They were then rinsed in deionized water (DI) for 5 minutes followed by 1 minute in DI:HCl (10:1). Lastly, the substrates were rinsed in DI water for 5 minutes and blown dry with filtered nitrogen.

Ablation was performed with a KrF excimer laser. The 248 nm illumination was focused to a typical spot size of 7 mm x 3 mm on a one inch diameter, 95% dense YBCO target. The energy density at the target was 0.8 J cm^{-2}. The laser beam was incident at 45°. The target was rotated at 7 rpm and the laser spot was scanned from the centre to the edge of the target with a period of 65 s. The substrate was mounted with silver paste on a three inch diameter heater located 6 cm away from the target. Depositions were performed with a laser pulse rate of two per second. After the sample was loaded, the vacuum chamber was evacuated to 5×10^{-7} Torr while the substrate was heated to the deposition temperature, which was controlled through a thermocouple embedded in the heater. Oxygen was introduced to the chamber to a pressure of 170 mTorr during deposition. The duration of the depositions was typically one hour. After the deposition, the temperature of the heater was ramped down to 450° C at a rate of 2° C min^{-1} while the oxygen pressure was increased to 1 atm. The substrates were held at this temperature for 2 hours and then ramped down at a rate of 2° C min^{-1}.

Following the deposition of the films, their resistance was measured as a function of temperature. This measurement was done in a closed cycle cryostat using a four-probe method. One micron diameter gold wires were ultrasonically bonded directly to the surface of the superconductor for these measurements. A constant current of 0.1 mA was passed through the two outer leads while the voltage across the inner two leads was measured.

For measurement of the critical current density (J_c), the films were patterned into a 10 μm and 5 μm wide, 2.77 mm long meander test structure. Positive photolithography was used to form the structure on the superconductor films using Shipley 1400-31 positive photoresist. The YBCO films were etched in DI:H_3PO_4 (100:1).

Lift-off photolithography was employed to form metal contacts on the superconductor. Patterns were formed with Shipley AZ1400-37 photoresist. A 15 minute soak in chlorobenzene prior to development was used to form a reentrant photoresist profile for the lift-off. After deposition of 0.7 μm of silver and 0.3 μm of gold, a 15 minute soak in N-methyl-2-pyrrolidone was used to swell the photoresist. The lift-off of the excess metal was completed by soaking the samples in warm acetone for 10 minutes. 1 μm diameter gold wire was bonded to the metal contacts for electrical connections. The resistance versus temperature of the patterned test structure was measured using 1 μA of current. Below the critical temperature (T_c), the critical current was measured by increasing the amount of the current to the sample until the measured voltage exceeded the 1 μV cm^{-1} criteria.

YBCO films on 1 cm x 1 cm substrates were patterned into ring resonators by standard photolithographic steps as described above. The geometry of the resonator is shown in figure 1. The dimensions were: width of the microstrip (w) = 99 μm, gap size

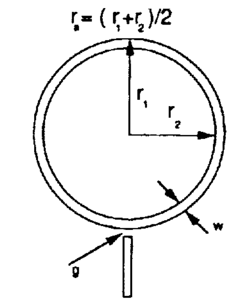

Figure 1. Layout of the microstrip ring resonator.

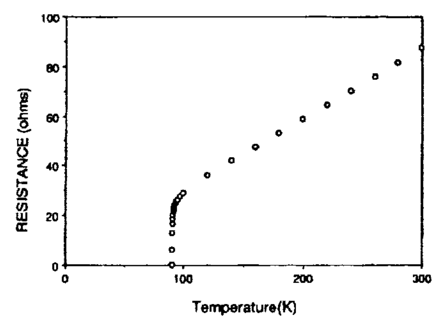

Figure 2. Resistance as a function of temperature of sample F.

(g) = 27 μm, substrate thickness (h) = 508 μm, and average radius = 2.45 mm. It had a characteristic impedance of 50 Ω and a fundamental resonant frequency of 5 GHz. Microwave measurements were performed at the first harmonic. The ground plane consisted of a 2.5 μm thick layer of gold on the back of the substrate. A resonator was also fabricated using 2.8 μm thick gold transmission lines for comparison.

3. Results

YBCO films were deposited on to seven $NdGaO_3$ substrates at five different substrate temperatures. X-ray diffraction spectroscopy showed the films to be epitaxial with the c axis perpendicular to the surface of the substrate. Table 1 lists the deposition temperatures, film thicknesses, critical temperatures before and after patterning, and critical current densities at 77 K. Samples A to E were patterned for critical current density measurements. The critical current densities of samples F and G were not measured since they were patterned into ring resonators. Figure 2 shows the resistance as a function of temperature for sample F after patterning. The critical temperature of this film was 89.7 K and the transition width was 1 K.

From table 1 it can be seen that the critical temperature after patterning is usually slightly higher than that before patterning. This is probably a result of non-uniformity in the film and the location of the measurement. Prior to patterning, the measurements were

Table 1. Deposition temperature and DC properties of YBCO films.

Sample	T_d (°C)	T_c (K) before	T_c (K) after	t (μm)	$J_c \times 10^{-8}$ (A cm^{-2})
A	715	87.1	88.3	0.37	1.50
B	735	87.9	88.5	0.26	0.22
C	745	88.0	89.1	0.35	2.25
D	755	87.4	86.6	0.38	0.45
E	785	—	87.5	0.24	0.44
F	785	88.6	89.7	0.30	resonator
G	785	87.8	87.3	0.38	resonator

performed by wire bonding directly to the films with the contacts located near the edge of the sample to prevent mechanical damage in the centre. The patterned test structures, on the other hand, were located near the centre of the samples suggesting that the quality of the films was higher near the centres than at the edges. Sample D was unintentionally over etched. Its critical temperature showed a decrease after patterning.

If the samples are ranked according to critical temperature after patterning it can be seen that, with the exception of sample B, higher critical current densities correspond to higher critical temperatures. Sample B, which had a relatively high critical temperature, also had the lowest critical current density. Inspection of this sample with an optical microscope revealed a large particle in the 10 μm wide YBCO line used for the critical current density measurement. This probably accounts for the anomalously low J_c.

The scattering parameters of the ring resonators fabricated on samples F and G were measured as a function of temperature. The magnitude of S_{11} is plotted as a function of frequency for sample G at 79 K in figure 3, showing the resonance at 10.14 GHz. The unloaded quality factor of the resonance was determined from the S_{11} data using the 3 dB frequencies, resonant frequency, reflection coefficients on and off resonance and phase information to account for the coupling coefficient and coupling losses. The details of the technique are describe elsewhere [12–14]. The unloaded quality factors (Q_0) were determined as a function of temperature for samples F and G at 10 GHz. At 77 K they had unloaded quality factors of 326 and 876 respectively. Note that although sample F had a higher critical temperature, sample G had better microwave performance. This is probably a result of surface morphology. A rough film will exhibit more loss than a smooth film with otherwise identical properties [15]. The surface of sample F had cloudy spots, which we have correlated with roughness by optical and scanning electron microscopy on other samples.

The unloaded quality factors of samples F and G are plotted as a function of temperature in figure 4. As expected, Q_0 increases rapidly as the temperature is decreased below T_c. However, as the temperature is further decreased Q_0 reaches a maximum and then decreases. This is particularly apparent in sample G, which had the higher Q_0. This phenomenon was observed when the measurement was performed with either increasing or decreasing temperatures. The measurements were repeatable. This is quite different from the expected behaviour, such as observed for YBCO resonators on $LaAlO_3$ substrates, for which Q_0 tends to levels off but not decrease at low temperatures. This suggests that the losses in the $NdGaO_3$ substrate increase as the temperature is decreased.

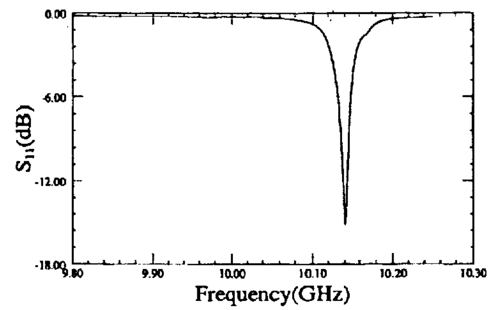

Figure 3. Magnitude of S_{11} as a function of frequency for the ring resonator patterned from film G measured at 79 K.

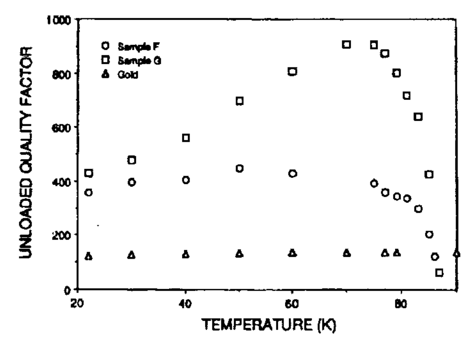

Figure 4. Unloaded quality factors at 10 GHz of samples F (circles) and G (squares) and the gold resonator (triangles) from 20 K to room temperature.

To verify that the decrease in the quality factor is due to the substrate and not due to the properties of YBCO on $NdGaO_3$, the reflection coefficient for a gold resonator on $NdGaO_3$ was also measured from 20 K to room temperature. The results of this measurement are shown in figure 5. The decrease in Q_0 at low temperatures was observed here as well. To facilitate comparison with the superconducting resonators, the data for the gold resonator below 90 K are also plotted in figure 4.

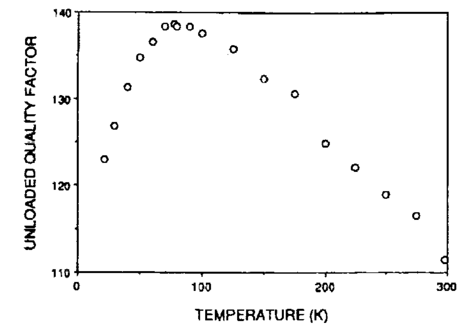

Figure 5. Unloaded quality factor at 10 GHz of the gold resonator from 20 K to room temperature.

4. Discussion

To determine the surface resistance of the YBCO films, the losses in the substrate and to radiation must be accounted for. The loss by radiation is assumed to be negligible due to shielding of the circuit. The losses in the dielectric are clearly not negligible, however, especially at low temperature. We have attempted to extract the losses in the dielectric from the measurements on the gold resonator by three techniques. The first two were not successful. For the first technique we calculated the expected conductor quality factor from measured DC values of the resistivity of thin films of gold. For the second technique we used conductor quality factors obtained by scaling values measured at 35 GHz, reported in reference [14], to 10 GHz. The loss tangent of the dielectric was then calculated from the unloaded quality factor of the gold resonator using

$$\tan\delta = \frac{1}{Q_d} = \frac{1}{Q_{oAu}} - \frac{1}{Q_{cAu}} \qquad (1)$$

where $\tan\delta$ is the loss tangent, Q_d is the dielectric quality factor and Q_0 and Q_c are the unloaded quality factor and conductor quality factor respectively. The loss tangent is actually proportional to $1/Q_d$ but the constant of proportionality is very near unity in this case and is assumed to be unity hereafter. Both of these techniques produced values of $\tan\delta$ that implied greater loss in the dielectric than the total measured loss for samples F and G, that is $Q_d < Q_0$, which is inconsistant. This is most probably due to the difficulty in scaling the surface resistance of gold for the frequency changes since the effects of non-idealities such as surface roughness were neglected.

The data shown in figure 4 suggest that near T_c the losses are dominated by those in the superconductor while at low temperatures the losses in the substrate dominate. We can take advantage of this to help separate the two components of the loss. Young *et al* have reported $\tan\delta = 3 \times 10^{-4}$ for $NdGaO_3$ at 77 K [11] and 5 GHz. We have used this value as a starting point in an iterative technique for extracting the temperature dependence of the loss tangent from the unloaded quality factors of sample G and the gold resonator. The technique basically consists of the following steps.

(i) Extrapolate the conductor loss at low temperature from its value at 77 K.

(ii) Estimate the dielectric loss below 70 K, where it is dominant, from the unloaded quality factor and the extrapolated conductor loss.

(iii) Use a curve fit to extrapolate the dielectric loss above 77 K to T_c.

(iv) Use the extrapolated dielectric loss to recalculate the conductor loss between 77 K and T_c and use a curve fit to refine the estimate of the conductor loss from 0 K to T_c.

(v) Use the refined estimate of conductor loss to redetermine the dielectric loss from 0 K to T_c.

(vi) Compare the resulting dielectric loss tangent at 77 K to the reported value of 3×10^{-4}, adjust the initial estimate of conductor loss at 77 K, and repeat the process.

The extrapolation of conductor loss is based on the two-fluid model for losses in superconductors while the extrapolation of dielectric loss is based on a fit to an exponential. A detailed description of the procedure follows. The values reported in the description are for the final iteration of the process.

Using a starting estimate of 4.4×10^{-4} for the loss tangent (3×10^{-4} for the first iteration), the conductor quality factor for sample G at 77 K is found to be 1425 through equation (1). The quality factor of the superconducting resonator varies little for temperatures sufficiently below T_c. (77 K is not quite far enough below T_c. This accounts for the difference between the starting estimate of 4.4×10^{-4} for the final iteration and the value of 3×10^{-4} with results at the end of the iteration.) Assuming Q_{cG}, the conductor quality factor of sample G, has a value equal to that at 77 K for all lower temperatures allows determination of a first estimate of the loss tangent of the substrate. It is shown on a semi-logarithmic plot in figure 6. The loss tangent was found to fit quite well

$$\tan\delta = K e^{-\gamma T} \qquad (2)$$

over this temperature range. T is the absolute temperature and K and γ are fitting parameters. The results of the fit were used to extrapolate the loss tangent above 77 K to T_c. The conductor quality factor is changing rapidly above 77 K, where the subtractive approach of equation (1) assuming Q_c constant would be invalid.

The loss tangents calculated from this fit were then used in equation (1) to extract an estimate of Q_{cAu} the conductor quality factor of the gold resonator, as a function of temperature. An estimate of the surface resistance of the gold films, R_{sAu}, was calculated from Q_{cAu} through equation (3) [16, 17].

$$R_{sAu} = \frac{4\pi Z_0}{B(2C + D)} \frac{\pi}{\lambda} \left(\frac{1}{Q_{cAu}}\right) \qquad (3)$$

$$B = 1 - \left(\frac{w'}{4h}\right)^2 \qquad (4)$$

$$C = \left(1 - \frac{t}{\pi w'}\right) \Big/ h \qquad (5)$$

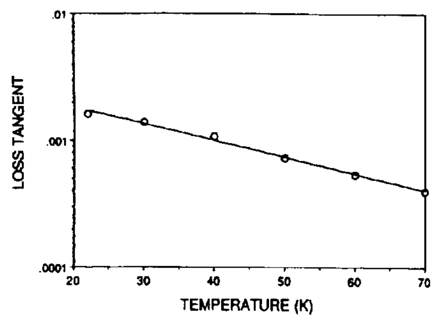

Figure 6. First estimate of the loss tangent of $NdGaO_3$ from 20 K to 70 K obtained by assuming the conductor quality factor of sample G is constant below 77 K. The circles are the data and the full line is the exponential fit.

$$D = 2\left(\pi + \ln\left(\frac{2h}{t}\right)\right) \Big/ \pi w' \tag{6}$$

$$w' = w + \frac{t}{\pi}\left(\ln\left(\frac{2h}{t}\right) + 1\right). \tag{7}$$

Z_0 is the characteristic impedence of the microstrip, λ is the guided wavelength and t is the thickness of the gold film.

Using equation (1) with the gold resonator and sample G we can write

$$\frac{1}{Q_{cG}} = \frac{1}{Q_{cAu}} - \left(\frac{1}{Q_{oAu}} - \frac{1}{Q_{oG}}\right) \tag{8}$$

Also, for a superconducting microstrip with a gold ground plane we have

$$\frac{1}{Q_{cG}} = \frac{\lambda}{\pi}\alpha_{cG} = \frac{\lambda}{\pi}\frac{B'\left((C'+D')\,R_{sG} + C'R_{sAu}\right)}{4\pi Z_0} \tag{9}$$

where α_{cG} is the conductor loss in sample G, R_{sG} is the effective surface resistance of the superconductor in sample G and B', C' and D' are determined from equations (4) to (7) using the thickness of the superconductor in sample G. Combining equations (3), (8) and (9) yields

$$R_{sG} = \left(\frac{B(2C+D) - B'C'}{B'(C'+D')}\right) R_{sAu} - \frac{4\pi Z_0}{B'(C'+D')}\frac{\pi}{\lambda}\left(\frac{1}{Q_{oAu}} - \frac{1}{Q_{oG}}\right) \tag{10}$$

which was used to estimate the effective surface resistance of the superconductor in sample G. The surface resistance calculated here is an effective value since corrections for the actual current distribution in the superconductor are not made [18].

A fit to the effective surface resistance thus determined was performed using the following equation

$$R_{sG} = R_0 + A\,(T/T_c)^4 \Big/ \left(1 - (T/T_c)^4\right)^{3/2} = R_0 + A f(\tau). \tag{11}$$

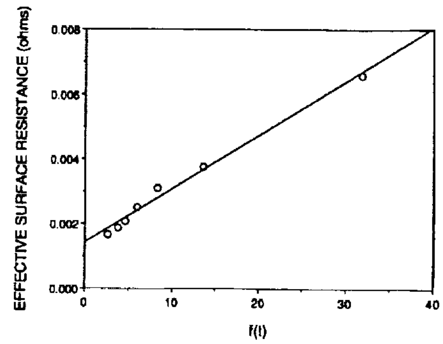

Figure 7. Effective surface resistance of sample G between 70 and 85 K calculated using the exponential from the curve fit of figure 6 to account for dielectric losses. The circles show the data and the line is the fit to the data using the two fluid model. See equation (11) for the definition of $f(\tau)$.

The first term, R_0, is a residual surface resistance, the second term is the surface resistance from the two fluid model [19] and $\tau = T/T_c$. The fitting parameters were R_0 and A. The effective surface resistances determined from equation (10) are shown in figure 7. The line shows the result of the fit. The data points shown correspond to temperatures from 70 to 85 K, the region in which the effective surface resistance is rapidly changing and the losses are dominated by the superconductor. The effective surface resistances at lower temperatures were not included to minimize the influence of errors in the estimation of the dielectric losses. The dielectric losses are large at low temperatures, and errors there could dominate the results of the fit. While equation (11) oversimplifies the temperature dependence of the surface resistance near T_c, where the pentration depth and the film thickness are comparable, it does allow an improvement in the extraction of $\tan\delta$ at low temperatures. The results of this fit are used to include the temperature dependence of Q_{cG} below 77 K, which was previously assumed constant.

Equation (10) was used to recalculate the surface resistance of gold using R_{sG} calculated from the fit and the measured values for Q_{oAu} and Q_{oG}. New values for the conductor quality factor for the gold resonator were then calculated using equation (3). Finally equation (1) was used to determine the loss tangent as a function of temperature. The value at 77 K was compared with 3×10^{-4} and, if needed, an adjustment to the original estimate of the conductor quality factor of sample G at 77 K was made and another iteration was performed. Figure 8 shows the loss tangent of $NdGaO_3$ as a function of temperature after the final iteration. The loss tangent is seen to increase by more than a factor of five from 77 K to 22 K.

The effective surface resistance of sample F was calculated using equation (10). The effective surface resistances for both superconducting resonators and the surface resistance of the gold resonator are plotted as a function of temperature in figure 9.

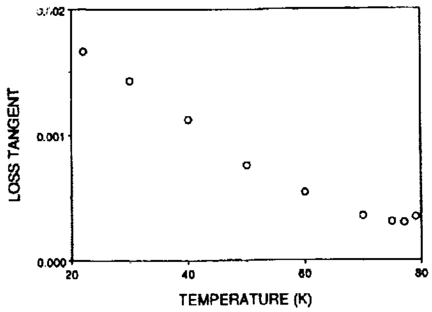

Figure 8. Loss tangent of $NdGaO_3$ from 20 K to 80 K extracted from the 10 GHz measurements on superconducting resonator G and the gold resonator.

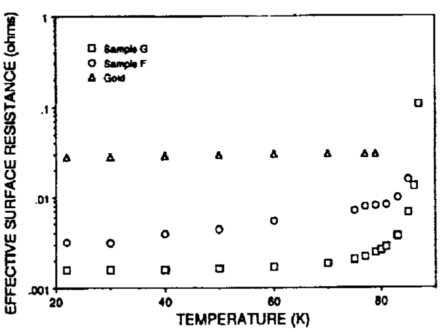

Figure 9. Effective surface resistance at 10 GHz as a function of temperature for superconducting resonators F (circles) and G (squares) and the gold resonator (triangles).

5. Conclusions

$YBa_2Cu_3O_{7-\delta}$ thin films were formed on $NdGaO_3$ substrates by laser ablation. The best films had critical temperatures greater than 89 K and critical current densities exceeding 2×10^6 A cm^{-2} at 77 K. Two films were patterned into microstrip ring resonators with gold ground planes. The better of the two resonators had an unloaded quality factor of 876 at 77 K, which was six times larger than that of a gold resonator of identical geometry. The unloaded quality factor increased to 910 at 70 K but then decreased as the temperature was further lowered. Qualitatively similar temperature dependence was observed for the gold resonator indicating that the losses at low temperature were being dominated by dielectric losses in the substrate.

The temperature dependence of the loss tangent was extracted from the measured quality factors of the gold and superconducting resonators for temperatures from 22 K to 80 K. The method employed to extract the temperature dependence of the loss tangent uses a previously reported value of 3×10^{-4} at 77 K [11]. The loss tangent was found to increase from 3×10^{-4} at 77 K to 1.7×10^{-3} at 22 K. These loss tangents are large compared to those for $LaAlO_3$, particularly at low temperatures, and $LaAlO_3$ is a better substrate than $NdGaO_3$ for microwave applications of high-temperature superconductors.

Acknowledgments

The authors are grateful to Mr Norman Rohrer for his assistance with the microwave measurements. This research was supported by the National Aeronautics and Space Administration under Award No. NCC-3-197.

References

[1] Laibowitz R B, Koch R H, Chaudhari P and Gambino R J 1987 *Phys. Rev.* B **35** 8822

[2] Simon R W, Platt C E, Lee A E, Lee G S, Daly K P, Wire M S, Laine J A and Urbanik M 1988 *Appl. Phys. Lett.* **53** 2677

[3] Samara G A, 1990 *J. Appl. Phys.* **68** 4214

[4] O'Bryan H M, Gallagher P K, Berkstresser G W and Brandle C D 1990 *J. Mater. Res.* **5** 183

[5] *Synoptics, Synthetic Crystal and Optical Products Data sheet*

[6] Giess E A *et al* 1990 *IBM J. Res. Develop.* **34** 916

[7] Sasaura M, Miyazawa S and Mukaida M 1990 *J. Appl. Phys.* **68** 3643

[8] Phillips J M, Siegal M S, Perry C L and Marshall J H 1991 *IEEE Trans. Magn.* **27** 1006

[9] Koren G, Gupta A, Giess E A, Segmiller A and Laibowitz R B 1989 *Appl. Phys. Lett.* **54** 1054

[10] Mukaida M, Miyazawa S, Sasaura M and Kuroka K 1990 *Japan. J. Appl. Phys.* **29** L936

[11] Young K H, Negrete G V, Sun J Z and James T W 1991 *Japan. J. Appl. Phys.* **30** L1355

[12] Romanofsky R R 1989 *NASA Technical Paper* TM-2899

[13] Rohrer N J, To H Y, Valco G J, Bhasin K B, Chorey C M and Warner J D 1990 *Science and Technology of Thin Film Superconductors* 2 (New York: Plenum) p 615

[14] Chorey C M, Kong K S, Bhasin K B, Warner J D and Itoh T 1991 *IEEE Trans. Microwave Theory Tech.* MTT-**39** 1480

[15] Valco G J, Blemker A R and Bhasin K B 1992 *Microwave and Optical Technology Letters*

[16] Takamoto J, Oshita F and Fetterman H 1989 *IEEE Trans. Microwave Theory Tech.* MTT-**37** 1650

[17] Pucel R A, Masse D J and Hartwig C P 1968 *IEEE Trans Microwave Theory Tech.* MTT-**16** 342

[18] Sheen D M, Ali S M, Oates D E, Withers R S and Kong J A 1991 *IEEE Trans. Appl. Supercond.* ASC-**1** 108

[19] Van Duzer T and Turner C W 1981 *Principles of Superconductive Devices and Circuits* (New York: Elsevier) p 131